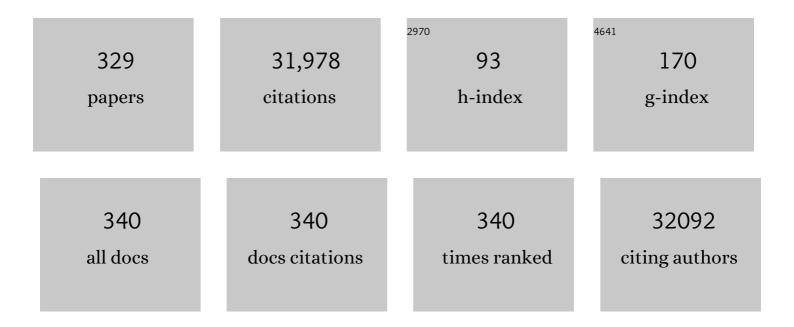
List of Publications by Year in descending order

Source: https://exaly.com/author-pdf/2076490/publications.pdf Version: 2024-02-01



#	Article	IF	CITATIONS
1	Above-bandgap voltages from ferroelectric photovoltaic devices. Nature Nanotechnology, 2010, 5, 143-147.	15.6	1,496
2	Unusual properties of the fundamental band gap of InN. Applied Physics Letters, 2002, 80, 3967-3969.	1.5	1,380
3	Three-dimensional nanopillar-array photovoltaics on low-cost and flexible substrates. Nature Materials, 2009, 8, 648-653.	13.3	997
4	Near-unity photoluminescence quantum yield in MoS <sub>2</sub> . Science, 2015, 350, 1065-1068.	6.0	993
5	Tailoring Copper Nanocrystals towards C <sub>2</sub> Products in Electrochemical CO <sub>2</sub> Reduction. Angewandte Chemie - International Edition, 2016, 55, 5789-5792.	7.2	667
6	Hydrolysis of Electrolyte Cations Enhances the Electrochemical Reduction of CO <sub>2</sub> over Ag and Cu. Journal of the American Chemical Society, 2016, 138, 13006-13012.	6.6	640
7	Superior radiation resistance of In1â^'xGaxN alloys: Full-solar-spectrum photovoltaic material system. Journal of Applied Physics, 2003, 94, 6477-6482.	1.1	572
8	Strain-Induced Indirect to Direct Bandgap Transition in Multilayer WSe <sub>2</sub> . Nano Letters, 2014, 14, 4592-4597.	4.5	572
9	Small band gap bowing in In1â^'xGaxN alloys. Applied Physics Letters, 2002, 80, 4741-4743.	1.5	563
10	Experimental demonstrations of spontaneous, solar-driven photoelectrochemical water splitting. Energy and Environmental Science, 2015, 8, 2811-2824.	15.6	520
11	Photovoltaic effects in BiFeO3. Applied Physics Letters, 2009, 95, .	1.5	460
12	The true toughness of human cortical bone measured with realistically short cracks. Nature Materials, 2008, 7, 672-677.	13.3	453
13	Temperature dependence of the fundamental band gap of InN. Journal of Applied Physics, 2003, 94, 4457-4460.	1.1	375
14	Quantitative measurement of residual biaxial stress by Raman spectroscopy in diamond grown on a Ti alloy by chemical vapor deposition. Physical Review B, 1993, 48, 2601-2607.	1.1	372
15	Electronic Structure of Monoclinic BiVO <sub>4</sub> . Chemistry of Materials, 2014, 26, 5365-5373.	3.2	356
16	Solid-state quantum memory using the 31P nuclear spin. Nature, 2008, 455, 1085-1088.	13.7	351
17	Efficient Photovoltaic Current Generation at Ferroelectric Domain Walls. Physical Review Letters, 2011, 107, 126805.	2.9	346
18	Age-related changes in the plasticity and toughness of human cortical bone at multiple length scales. Proceedings of the National Academy of Sciences of the United States of America, 2011, 108, 14416-14421	3.3	325

 $\mathsf{JOEL}\,\mathsf{W}\,\mathsf{AGER}$ 

#	Article	IF	CITATIONS
19	Transparent Electrodes for Efficient Optoelectronics. Advanced Electronic Materials, 2017, 3, 1600529.	2.6	310
20	Goldâ€Mediated Exfoliation of Ultralarge Optoelectronicallyâ€Perfect Monolayers. Advanced Materials, 2016, 28, 4053-4058.	11.1	307
21	Stability of Residual Oxides in Oxideâ€Derived Copper Catalysts for Electrochemical CO <sub>2</sub> Reduction Investigated with <sup>18</sup> O Labeling. Angewandte Chemie - International Edition, 2018, 57, 551-554.	7.2	300
22	Spatially resolved Raman studies of diamond films grown by chemical vapor deposition. Physical Review B, 1991, 43, 6491-6499.	1.1	288
23	Nature of room-temperature photoluminescence in ZnO. Applied Physics Letters, 2005, 86, 191911.	1.5	274
24	Photoactuators and motors based on carbon nanotubes with selective chirality distributions. Nature Communications, 2014, 5, 2983.	5.8	269
25	High Photoluminescence Quantum Yield in Band Gap Tunable Bromide Containing Mixed Halide Perovskites. Nano Letters, 2016, 16, 800-806.	4.5	269
26	Hardness, elastic modulus, and structure of very hard carbon films produced by cathodicâ€arc deposition with substrate pulse biasing. Applied Physics Letters, 1996, 68, 779-781.	1.5	255
27	Optimizing C–C Coupling on Oxide-Derived Copper Catalysts for Electrochemical CO <sub>2</sub> Reduction. Journal of Physical Chemistry C, 2017, 121, 14191-14203.	1.5	254
28	Exceptionally active iridium evolved from a pseudo-cubic perovskite for oxygen evolution in acid. Nature Communications, 2019, 10, 572.	5.8	254
29	Strain-engineered growth of two-dimensional materials. Nature Communications, 2017, 8, 608.	5.8	253
30	pâ€Type InP Nanopillar Photocathodes for Efficient Solarâ€Driven Hydrogen Production. Angewandte Chemie - International Edition, 2012, 51, 10760-10764.	7.2	245
31	Thin-Film Materials for the Protection of Semiconducting Photoelectrodes in Solar-Fuel Generators. Journal of Physical Chemistry C, 2015, 119, 24201-24228.	1.5	245
32	Electrical suppression of all nonradiative recombination pathways in monolayer semiconductors. Science, 2019, 364, 468-471.	6.0	243
33	Surface Composition Dependent Ligand Effect in Tuning the Activity of Nickel–Copper Bimetallic Electrocatalysts toward Hydrogen Evolution in Alkaline. Journal of the American Chemical Society, 2020, 142, 7765-7775.	6.6	234
34	Effect of Si doping on strain, cracking, and microstructure in GaN thin films grown by metalorganic chemical vapor deposition. Journal of Applied Physics, 2000, 87, 7745-7752.	1.1	233
35	Indirect Bandgap and Optical Properties of Monoclinic Bismuth Vanadate. Journal of Physical Chemistry C, 2015, 119, 2969-2974.	1.5	233
36	Recombination Kinetics and Effects of Superacid Treatment in Sulfur- and Selenium-Based Transition Metal Dichalcogenides. Nano Letters, 2016, 16, 2786-2791.	4.5	233

#	Article	IF	CITATIONS
37	Structure and electronic properties of InN and In-rich group III-nitride alloys. Journal Physics D: Applied Physics, 2006, 39, R83-R99.	1.3	229
38	Nature of the fundamental band gap in GaNxP1â^'x alloys. Applied Physics Letters, 2000, 76, 3251-3253.	1.5	228
39	Pressure Induced Deep Gap State of Oxygen in GaN. Physical Review Letters, 1997, 78, 3923-3926.	2.9	223
40	Evidence for product-specific active sites on oxide-derived Cu catalysts for electrochemical CO2 reduction. Nature Catalysis, 2019, 2, 86-93.	16.1	212
41	Investigating the Role of Copper Oxide in Electrochemical CO <sub>2</sub> Reduction in Real Time. ACS Applied Materials & Interfaces, 2018, 10, 8574-8584.	4.0	207
42	Efficient and Sustained Photoelectrochemical Water Oxidation by Cobalt Oxide/Silicon Photoanodes with Nanotextured Interfaces. Journal of the American Chemical Society, 2014, 136, 6191-6194.	6.6	204
43	Air-Stable n-Doping of WSe <sub>2</sub> by Anion Vacancy Formation with Mild Plasma Treatment. ACS Nano, 2016, 10, 6853-6860.	7.3	202
44	Photocatalytic Stability of Single- and Few-Layer MoS <sub>2</sub> . ACS Nano, 2015, 9, 11302-11309.	7.3	197
45	Interaction of Localized Electronic States with the Conduction Band: Band Anticrossing in II-VI Semiconductor Ternaries. Physical Review Letters, 2000, 85, 1552-1555.	2.9	195
46	Life-cycle net energy assessment of large-scale hydrogen production via photoelectrochemical water splitting. Energy and Environmental Science, 2014, 7, 3264-3278.	15.6	195
47	Raman Spectroscopy and Time-Resolved Photoluminescence of BN and BxCyNzNanotubes. Nano Letters, 2004, 4, 647-650.	4.5	194
48	Evidence forp-Type Doping of InN. Physical Review Letters, 2006, 96, 125505.	2.9	193
49	Spin pinning effect to reconstructed oxyhydroxide layer on ferromagnetic oxides for enhanced water oxidation. Nature Communications, 2021, 12, 3634.	5.8	186
50	Hardness and fracture toughness of bulk single crystal gallium nitride. Applied Physics Letters, 1996, 69, 4044-4046.	1.5	182
51	Measurement of the toughness of bone: A tutorial with special reference to small animal studies. Bone, 2008, 43, 798-812.	1.4	180
52	Fano interference of the Raman phonon in heavily boronâ€doped diamond films grown by chemical vapor deposition. Applied Physics Letters, 1995, 66, 616-618.	1.5	177
53	Synthetic Insertion of Gold Nanoparticles into Mesoporous Silica. Chemistry of Materials, 2003, 15, 1242-1248.	3.2	175
54	Wide bandgap BaSnO3 films with room temperature conductivity exceeding 104 S cmâ^'1. Nature Communications, 2017, 8, 15167.	5.8	175

#	Article	IF	CITATIONS
55	A spongy nickel-organic CO <sub>2</sub> reduction photocatalyst for nearly 100% selective CO production. Science Advances, 2017, 3, e1700921.	4.7	175
56	On the effect of X-ray irradiation on the deformation and fracture behavior of human cortical bone. Bone, 2010, 46, 1475-1485.	1.4	171
57	Electrochemical CO Reduction Builds Solvent Water into Oxygenate Products. Journal of the American Chemical Society, 2018, 140, 9337-9340.	6.6	170
58	Osteopontin deficiency increases bone fragility but preserves bone mass. Bone, 2010, 46, 1564-1573.	1.4	169
59	Effect of Si doping on the dislocation structure of GaN grown on the Aâ€face of sapphire. Applied Physics Letters, 1996, 69, 990-992.	1.5	166
60	Sequential catalysis controls selectivity in electrochemical CO <sub>2</sub> reduction on Cu. Energy and Environmental Science, 2018, 11, 2935-2944.	15.6	165
61	Encapsulation of Metal (Au, Ag, Pt) Nanoparticles into the Mesoporous SBA-15 Structure. Langmuir, 2003, 19, 4396-4401.	1.6	163
62	Reactive Sputtering of Bismuth Vanadate Photoanodes for Solar Water Splitting. Journal of Physical Chemistry C, 2013, 117, 21635-21642.	1.5	162
63	Optical properties and electronic structure of InN and In-rich group III-nitride alloys. Journal of Crystal Growth, 2004, 269, 119-127.	0.7	157
64	Effect of nitrogen on the band structure of GaInNAs alloys. Journal of Applied Physics, 1999, 86, 2349-2351.	1.1	153
65	Amorphous Si Thin Film Based Photocathodes with High Photovoltage for Efficient Hydrogen Production. Nano Letters, 2013, 13, 5615-5618.	4.5	151
66	Chemical storage of renewable energy. Science, 2018, 360, 707-708.	6.0	150
67	The Technical and Energetic Challenges of Separating (Photo)Electrochemical Carbon Dioxide Reduction Products. Joule, 2018, 2, 381-420.	11.7	148
68	Vitamin D Deficiency Induces Early Signs of Aging in Human Bone, Increasing the Risk of Fracture. Science Translational Medicine, 2013, 5, 193ra88.	5.8	146
69	Large-area and bright pulsed electroluminescence in monolayer semiconductors. Nature Communications, 2018, 9, 1229.	5.8	146
70	Efficient solar-driven electrochemical CO <sub>2</sub> reduction to hydrocarbons and oxygenates. Energy and Environmental Science, 2017, 10, 2222-2230.	15.6	145
71	Trace Levels of Copper in Carbon Materials Show Significant Electrochemical CO <sub>2</sub> Reduction Activity. ACS Catalysis, 2016, 6, 202-209.	5.5	143
72	CO <sub>2</sub> Electroreduction with Enhanced Ethylene and Ethanol Selectivity by Nanostructuring Polycrystalline Copper. ChemElectroChem, 2016, 3, 1012-1019.	1.7	142

#	Article	IF	CITATIONS
73	High Luminescence Efficiency in MoS <sub>2</sub> Grown by Chemical Vapor Deposition. ACS Nano, 2016, 10, 6535-6541.	7.3	140
74	Effects of temperature and gas–liquid mass transfer on the operation of small electrochemical cells for the quantitative evaluation of CO <sub>2</sub> reduction electrocatalysts. Physical Chemistry Chemical Physics, 2016, 18, 26777-26785.	1.3	138
75	Effects of substrate temperature on chemical structure of amorphous carbon films. Journal of Applied Physics, 1992, 71, 2243-2248.	1.1	133
76	Research advances towards large-scale solar hydrogen production from water. EnergyChem, 2019, 1, 100014.	10.1	130
77	Multiband GaNAsP quaternary alloys. Applied Physics Letters, 2006, 88, 092110.	1.5	128
78	Role of microstructure in the aging-related deterioration of the toughness of human cortical bone. Materials Science and Engineering C, 2006, 26, 1251-1260.	3.8	128
79	Role of TiO <sub>2</sub> Surface Passivation on Improving the Performance of p-InP Photocathodes. Journal of Physical Chemistry C, 2015, 119, 2308-2313.	1.5	127
80	p-Type Transparent Conducting Oxide/n-Type Semiconductor Heterojunctions for Efficient and Stable Solar Water Oxidation. Journal of the American Chemical Society, 2015, 137, 9595-9603.	6.6	122
81	The effect of aging on crack-growth resistance and toughening mechanisms in human dentin. Biomaterials, 2008, 29, 1318-1328.	5.7	121
82	Band Anticrossing in III-N-V Alloys. Physica Status Solidi (B): Basic Research, 2001, 223, 75-85.	0.7	119
83	Dependence of the fundamental band gap of AlxGa1â^'xN on alloy composition and pressure. Journal of Applied Physics, 1999, 85, 8505-8507.	1.1	112
84	Annealing studies of lowâ€ŧemperatureâ€grown GaAs:Be. Journal of Applied Physics, 1992, 71, 1699-1707.	1.1	111
85	Large Melting-Point Hysteresis of Ge Nanocrystals Embedded inSiO2. Physical Review Letters, 2006, 97, 155701.	2.9	108
86	Coherence of spin qubits in silicon. Journal of Physics Condensed Matter, 2006, 18, S783-S794.	0.7	107
87	General Thermal Texturization Process of MoS <sub>2</sub> for Efficient Electrocatalytic Hydrogen Evolution Reaction. Nano Letters, 2016, 16, 4047-4053.	4.5	106
88	Thermal stability of amorphous hard carbon films produced by cathodic arc deposition. Applied Physics Letters, 1997, 71, 3367-3369.	1.5	104
89	Universal bandgap bowing in group-III nitride alloys. Solid State Communications, 2003, 127, 411-414.	0.9	104
90	On the crystalline structure, stoichiometry and band gap of InN thin films. Applied Physics Letters, 2005, 86, 071910.	1.5	103

#	Article	IF	CITATIONS
91	Effect of intrinsic growth stress on the Raman spectra of vacuumâ€arcâ€deposited amorphous carbon films. Applied Physics Letters, 1995, 66, 3444-3446.	1.5	102
92	Reduction of band-gap energy in GaNAs and AlGaNAs synthesized by N+ implantation. Applied Physics Letters, 1999, 75, 1410-1412.	1.5	102
93	Moâ€Ðoped BiVO <sub>4</sub> Photoanodes Synthesized by Reactive Sputtering. ChemSusChem, 2015, 8, 1066-1071.	3.6	100
94	Light emission during fracture of a Zr–Ti–Ni–Cu–Be bulk metallic glass. Applied Physics Letters, 1999, 74, 3809-3811.	1.5	94
95	Si photocathode with Ag-supported dendritic Cu catalyst for CO <sub>2</sub> reduction. Energy and Environmental Science, 2019, 12, 1068-1077.	15.6	93
96	Reduced size-independent mechanical properties of cortical bone in high-fat diet-induced obesity. Bone, 2010, 46, 217-225.	1.4	90
97	Tailoring Copper Nanocrystals towards C <sub>2</sub> Products in Electrochemical CO <sub>2</sub> Reduction. Angewandte Chemie, 2016, 128, 5883-5886.	1.6	90
98	Chemical Bath Deposition of p-Type Transparent, Highly Conducting (CuS) <sub><i>x</i></sub> :(ZnS) <sub>1–<i>x</i></sub> Nanocomposite Thin Films and Fabrication of Si Heterojunction Solar Cells. Nano Letters, 2016, 16, 1925-1932.	4.5	89
99	Effects of polar solvents on the fracture resistance of dentin: role of water hydration. Acta Biomaterialia, 2005, 1, 31-43.	4.1	87
100	Local vibrational mode spectroscopy of nitrogenâ€hydrogen complex in ZnSe. Applied Physics Letters, 1993, 63, 2756-2758.	1.5	86
101	Highly Stable Near-Unity Photoluminescence Yield in Monolayer MoS <sub>2</sub> by Fluoropolymer Encapsulation and Superacid Treatment. ACS Nano, 2017, 11, 5179-5185.	7.3	86
102	Aging and fracture of human cortical bone and tooth dentin. Jom, 2008, 60, 33-38.	0.9	85
103	Robust production of purified H <sub>2</sub> in a stable, self-regulating, and continuously operating solar fuel generator. Energy and Environmental Science, 2014, 7, 297-301.	15.6	85
104	Investigation and mitigation of degradation mechanisms in Cu2O photoelectrodes for CO2 reduction to ethylene. Nature Energy, 2021, 6, 1124-1132.	19.8	85
105	Size-Dependent Polar Ordering in Colloidal GeTe Nanocrystals. Nano Letters, 2011, 11, 1147-1152.	4.5	84
106	Pressure-dependent photoluminescence study of ZnO nanowires. Applied Physics Letters, 2005, 86, 153117.	1.5	83
107	Synthetic WSe <sub>2</sub> monolayers with high photoluminescence quantum yield. Science Advances, 2019, 5, eaau4728.	4.7	78
108	BiVO <sub>4</sub> thin film photoanodes grown by chemical vapor deposition. Physical Chemistry Chemical Physics, 2014, 16, 1651-1657.	1.3	77

#	Article	IF	CITATIONS
109	Effect of oxygen on the electronic band structure in ZnOxSe1â^'x alloys. Applied Physics Letters, 2003, 83, 299-301.	1.5	76
110	Electron spin coherence of phosphorus donors in silicon: Effect of environmental nuclei. Physical Review B, 2010, 82, .	1.1	76
111	Changes in cortical bone response to high-fat diet from adolescence to adulthood in mice. Osteoporosis International, 2011, 22, 2283-2293.	1.3	76
112	Opportunities to improve the net energy performance of photoelectrochemical water-splitting technology. Energy and Environmental Science, 2016, 9, 803-819.	15.6	75
113	Copperâ€alloyed ZnS as a pâ€type transparent conducting material. Physica Status Solidi (A) Applications and Materials Science, 2012, 209, 2101-2107.	0.8	73
114	Structure Sensitivity of Vibrational Spectra of Mesoporous Silica SBA-15 and Pt/SBA-15. Journal of Physical Chemistry B, 2005, 109, 17386-17390.	1.2	71
115	Characterization of chemical bonding and physical characteristics of diamond-like amorphous carbon and diamond films. Journal of Materials Research, 1992, 7, 404-410.	1.2	70
116	Pressure dependence of the fundamental band-gap energy of CdSe. Applied Physics Letters, 2004, 84, 67-69.	1.5	70
117	Net primary energy balance of a solar-driven photoelectrochemical water-splitting device. Energy and Environmental Science, 2013, 6, 2380.	15.6	69
118	Particle―and photoinduced conductivity in typeâ€la diamonds. Journal of Applied Physics, 1993, 74, 1086-1095.	1.1	68
119	Band gap bowing parameter of In1â^'xAlxN. Journal of Applied Physics, 2008, 104, .	1.1	67
120	Hole transport and photoluminescence in Mg-doped InN. Journal of Applied Physics, 2010, 107, .	1.1	67
121	Local vibrational modes in Mg-doped gallium nitride. Physical Review B, 1994, 49, 14758-14761.	1.1	65
122	A direct thin-film path towards low-cost large-area III-V photovoltaics. Scientific Reports, 2013, 3, 2275.	1.6	65
123	Pressure–Temperature Phase Diagram of Vanadium Dioxide. Nano Letters, 2017, 17, 2512-2516.	4.5	65
124	Metal–Oxygen Hybridization Determined Activity in Spinel-Based Oxygen Evolution Catalysts: A Case Study of ZnFe <sub>2–<i>x</i></sub> Cr <sub><i>x</i></sub> O <sub>4</sub> . Chemistry of Materials, 2018, 30, 6839-6848.	3.2	65
125	Hydrogen-induced platelets in silicon: Infrared absorption and Raman scattering. Physical Review B, 1992, 45, 13363-13366.	1.1	64
126	Demonstration of a III–Nitride/Silicon Tandem Solar Cell. Applied Physics Express, 2009, 2, 122202.	1.1	64

#	Article	IF	CITATIONS
127	Al <sub>2</sub> O <sub>3</sub> Surface Complexation for Photocatalytic Organic Transformations. Journal of the American Chemical Society, 2017, 139, 269-276.	6.6	64
128	Sequential Cascade Electrocatalytic Conversion of Carbon Dioxide to C–C Coupled Products. ACS Applied Energy Materials, 2019, 2, 4551-4559.	2.5	64
129	Optical Detection and Ionization of Donors in Specific Electronic and Nuclear Spin States. Physical Review Letters, 2006, 97, 227401.	2.9	63
130	Wetting-regulated gas-involving (photo)electrocatalysis: biomimetics in energy conversion. Chemical Society Reviews, 2021, 50, 10674-10699.	18.7	63
131	Interface characterization of chemically vapor deposited diamond on titanium and Tiâ€6Alâ€4V. Journal of Applied Physics, 1993, 74, 7542-7550.	1.1	61
132	Current status of research and development of IIIÂNÂV semiconductor alloys. Semiconductor Science and Technology, 2002, 17, 741-745.	1.0	61
133	Temperature dependent mobility in singleâ€crystal and chemical vaporâ€deposited diamond. Journal of Applied Physics, 1993, 73, 2888-2894.	1.1	60
134	Effect of charged dislocation scattering on electrical and electrothermal transport in <mml:math xmlns:mml="http://www.w3.org/1998/Math/MathML" display="inline"&gt;<mml:mi>n</mml:mi>-type InN. Physical Review B, 2011, 84, .</mml:math 	1.1	59
135	The 2022 solar fuels roadmap. Journal Physics D: Applied Physics, 2022, 55, 323003.	1.3	58
136	Mgâ€doped InN and InGaN – Photoluminescence, capacitance–voltage and thermopower measurements. Physica Status Solidi (B): Basic Research, 2008, 245, 873-877.	0.7	55
137	Locus of pairing interaction inYBa2Cu3O7by site-selective oxygen isotope shift:O18inCuO2plane layers. Physical Review Letters, 1993, 70, 81-84.	2.9	54
138	Quantum-coupled radial-breathing oscillations in double-walled carbon nanotubes. Nature Communications, 2013, 4, 1375.	5.8	54
139	Solutionâ€Processed Transparent Selfâ€Powered p uSâ€ZnS/nâ€ZnO UV Photodiode. Physica Status Solidi - Rapid Research Letters, 2018, 12, 1700381.	1.2	54
140	Structure and mechanical properties of hydrogenated carbon films prepared by magnetron sputtering (for magnetic discs). IEEE Transactions on Magnetics, 1991, 27, 5160-5162.	1.2	53
141	Heat treatment of cathodic arc deposited amorphous hard carbon films. Thin Solid Films, 1997, 308-309, 186-190.	0.8	53
142	Electron emission from films of carbon nanotubes and ta-C coated nanotubes. Applied Physics Letters, 1999, 75, 2680-2682.	1.5	53
143	Quantifying van der Waals Interactions in Layered Transition Metal Dichalcogenides from Pressure-Enhanced Valence Band Splitting. Nano Letters, 2017, 17, 4982-4988.	4.5	53
144	Fatigue threshold R-curves for predicting reliability of ceramics under cyclic loading. Acta Materialia, 2005, 53, 2595-2605.	3.8	52

#	Article	IF	CITATIONS
145	Mechanism of stress relaxation in Ge nanocrystals embedded in SiO2. Applied Physics Letters, 2005, 86, 063107.	1.5	52
146	Undoped and Ni-Doped CoO <sub><i>x</i></sub> Surface Modification of Porous BiVO <sub>4</sub> Photoelectrodes for Water Oxidation. Journal of Physical Chemistry C, 2016, 120, 23449-23457.	1.5	52
147	Mapping materials properties with Raman spectroscopy utilizing a 2-D detector. Applied Optics, 1990, 29, 4969.	2.1	50
148	Enhancement of the photoelectrochemical water splitting by perovskite BiFeO3 via interfacial engineering. Solar Energy, 2020, 202, 198-203.	2.9	49
149	Raman and resistivity investigations of carbon overcoats of thinâ€film media: Correlations with tribological properties. Journal of Applied Physics, 1991, 69, 5748-5750.	1.1	48
150	Annealing of nonhydrogenated amorphous carbon films prepared by filtered cathodic arc deposition. Journal of Applied Physics, 2000, 88, 2395-2399.	1.1	48
151	Structural and electronic properties of amorphous and polycrystalline In2Se3 films. Journal of Applied Physics, 2003, 94, 2390-2397.	1.1	48
152	Manipulating Intermediates at the Au–TiO <sub>2</sub> Interface over InP Nanopillar Array for Photoelectrochemical CO <sub>2</sub> Reduction. ACS Catalysis, 2021, 11, 11416-11428.	5.5	48
153	On the Increasing Fragility of Human Teeth With Age: A Deep-UV Resonance Raman Study. Journal of Bone and Mineral Research, 2006, 21, 1879-1887.	3.1	47
154	Active Phase on SrCo <sub>1–<i>x</i></sub> Fe <sub><i>x</i></sub> O <sub>3â^îî</sub> (0 ≤i>x â‰ Perovskite for Water Oxidation: Reconstructed Surface versus Remaining Bulk. Jacs Au, 2021, 1, 108-115.	<b>0</b> .5) 3.6	47
155	Synthesis of InNxP1â^'x thin films by N ion implantation. Applied Physics Letters, 2001, 78, 1077-1079.	1.5	46
156	Phosphate tuned copper electrodeposition and promoted formic acid selectivity for carbon dioxide reduction. Journal of Materials Chemistry A, 2017, 5, 11905-11916.	5.2	46
157	The degree of bone mineralization is maintained with single intravenous bisphosphonates in aged estrogen-deficient rats and is a strong predictor of bone strength. Bone, 2007, 41, 804-812.	1.4	45
158	Direct growth of single-crystalline III–V semiconductors on amorphous substrates. Nature Communications, 2016, 7, 10502.	5.8	45
159	Control of Defect Concentrations within a Semiconductor through Adsorption. Physical Review Letters, 2006, 97, 055503.	2.9	44
160	Mg doped InN and confirmation of free holes in InN. Applied Physics Letters, 2011, 98, 042104.	1,5	44
161	Stability of Residual Oxides in Oxideâ€Derived Copper Catalysts for Electrochemical CO 2 Reduction Investigated with 18 O Labeling. Angewandte Chemie, 2018, 130, 560-563.	1.6	43
162	Formation of diluted III–V nitride thin films by N ion implantation. Journal of Applied Physics, 2001, 90, 2227-2234.	1.1	42

#	Article	IF	CITATIONS
163	Optical characterization of sputtered carbon films (magnetic media overlayers). IEEE Transactions on Magnetics, 1993, 29, 259-263.	1.2	41
164	Heterogenized Pyridine-Substituted Cobalt(II) Phthalocyanine Yields Reduction of CO <sub>2</sub> by Tuning the Electron Affinity of the Co Center. ACS Applied Materials & Interfaces, 2020, 12, 5251-5258.	4.0	41
165	Lattice site–dependent metal leaching in perovskites toward a honeycomb-like water oxidation catalyst. Science Advances, 2021, 7, eabk1788.	4.7	41
166	Pâ€Type Transparent Cuâ€Alloyed ZnS Deposited at Room Temperature. Advanced Electronic Materials, 2016, 2, 1500396.	2.6	40
167	Fracture and Ageing in Bone: Toughness and Structural Characterization. Strain, 2006, 42, 225-232.	1.4	39
168	Alkali Additives Enable Efficient Large Area (>55 cm <sup>2</sup> ) Slotâ€Die Coated Perovskite Solar Modules. Advanced Functional Materials, 2022, 32, .	7.8	39
169	Band-gap bowing effects in BxGa1â^'xAs alloys. Journal of Applied Physics, 2003, 93, 2696-2699.	1.1	38
170	Stable, freestanding Ge nanocrystals. Journal of Applied Physics, 2005, 97, 124316.	1.1	38
171	Optimization of Ge/C ratio for compensation of misfit strain in solid phase epitaxial growth of SiGe layers. Applied Physics Letters, 1993, 63, 2682-2684.	1.5	36
172	Band anticrossing in dilute nitrides. Journal of Physics Condensed Matter, 2004, 16, S3355-S3372.	0.7	34
173	High-Purity, Isotopically Enriched Bulk Silicon. Journal of the Electrochemical Society, 2005, 152, G448.	1.3	34
174	Direct observation of the donor nuclear spin in a near-gap bound exciton transition: P31 in highly enriched S28i. Journal of Applied Physics, 2007, 101, 081724.	1.1	34
175	The aminobisphosphonate risedronate preserves localized mineral and material properties of bone in the presence of glucocorticoids. Arthritis and Rheumatism, 2007, 56, 3726-3737.	6.7	34
176	Gas phase kinetics of the reactions of Na and NaO with O3 and N2O. Journal of Chemical Physics, 1986, 85, 5584-5592.	1.2	33
177	Diamond synthesis by microwave plasma chemical vapor deposition using graphite as the carbon source. Applied Physics Letters, 1991, 59, 2386-2388.	1.5	33
178	Direct evidence of carbon precipitates in GaAs and InP. Applied Physics Letters, 1994, 65, 1145-1147.	1.5	33
179	An Ultravioletâ `'Raman Spectroscopic Investigation of Magnesium Chlorideâ `'Ethanol Solids with a 0.47 to 6 Molar Ratio of C2H5OH to MgCl2. Journal of Physical Chemistry B, 2002, 106, 2946-2949.	1.2	33
180	Nonepitaxial Thin-Film InP for Scalable and Efficient Photocathodes. Journal of Physical Chemistry Letters, 2015, 6, 2177-2182.	2.1	33

#	Article	IF	CITATIONS
181	Al2O3scale development on iron aluminides. Journal of Materials Research, 2006, 21, 1409-1419.	1.2	32
182	Activation Effect of Electrochemical Cycling on Gold Nanoparticles towards the Hydrogen Evolution Reaction in Sulfuric Acid. Electrochimica Acta, 2016, 209, 440-447.	2.6	32
183	Hydrogen evolution activity of individual mono-, bi-, and few-layer MoS 2 towards photocatalysis. Applied Materials Today, 2017, 8, 132-140.	2.3	32
184	Band anticrossing in group II-Ox–VI1â^'x highly mismatched alloys: Cd1â^'xMnyOxTe1â^'x quaternaries synthesized by O ion implantation. Applied Physics Letters, 2002, 80, 1571-1573.	1.5	31
185	Probing and modulating surface electron accumulation in InN by the electrolyte gated Hall effect. Applied Physics Letters, 2008, 93, .	1.5	31
186	Pressurizing Field-Effect Transistors of Few-Layer MoS <sub>2</sub> in a Diamond Anvil Cell. Nano Letters, 2017, 17, 194-199.	4.5	31
187	A discussion on the possible involvement of singlet oxygen in oxygen electrocatalysis. JPhys Energy, 2021, 3, 031004.	2.3	31
188	Machine Learning Optimization of p-Type Transparent Conducting Films. Chemistry of Materials, 2019, 31, 7340-7350.	3.2	30
189	Nitrogen-induced enhancement of the free electron concentration in sulfur implanted GaNxAs1â^'x. Applied Physics Letters, 2000, 77, 2858-2860.	1.5	29
190	High electron mobility InN. Applied Physics Letters, 2007, 90, 162103.	1.5	29
191	Limitations and Advantages of Raman Spectroscopy for the Determination of Oxidation Stresses. Oxidation of Metals, 2011, 75, 229-245.	1.0	29
192	Carbon neutral manufacturing via on-site CO2 recycling. IScience, 2021, 24, 102514.	1.9	29
193	Gas phase kinetics of the reactions of NaO with H2, D2, H2O, and D2O. Journal of Chemical Physics, 1987, 87, 921-925.	1.2	27
194	Embedded Binary Eutectic Alloy Nanostructures: A New Class of Phase Change Materials. Nano Letters, 2010, 10, 2794-2798.	4.5	27
195	Rationally Designed, Threeâ€Ðimensional Carbon Nanotube Backâ€Contacts for Efficient Solar Devices. Advanced Energy Materials, 2011, 1, 1040-1045.	10.2	27
196	Few electron double quantum dot in an isotopically purified 28Si quantum well. Applied Physics Letters, 2012, 100, .	1.5	27
197	Multilayer hard carbon films with low wear rates. Surface and Coatings Technology, 1997, 91, 91-94.	2.2	26
198	Residual Stress in Diamond and Amorphous Carbon Films. Materials Research Society Symposia Proceedings, 1995, 383, 143.	0.1	25

#	Article	IF	CITATIONS
199	Narrow bandgap group III-nitride alloys. Physica Status Solidi (B): Basic Research, 2003, 240, 412-416.	0.7	25
200	Electrical properties of InGaNâ€6i heterojunctions. Physica Status Solidi C: Current Topics in Solid State Physics, 2009, 6, S413.	0.8	25
201	Gas phase studies of Na diffusion in He and Ar and kinetics of Na+Cl2and Na+SF6. Journal of Chemical Physics, 1986, 84, 6161-6169.	1.2	24
202	Nanoscale Probing of High Photovoltages at 109° Domain Walls. Ferroelectrics, 2012, 433, 123-126.	0.3	24
203	Economically viable CO <sub>2</sub> electroreduction embedded within ethylene oxide manufacturing. Energy and Environmental Science, 2021, 14, 1530-1543.	15.6	24
204	Laser heating effects in the characterization of carbon fibers by Raman spectroscopy. Journal of Applied Physics, 1990, 68, 3598-3608.	1.1	23
205	p-type InN and In-rich InGaN. Physica Status Solidi (B): Basic Research, 2007, 244, 1820-1824.	0.7	23
206	Spatially Precise Transfer of Patterned Monolayer WS <sub>2</sub> and MoS <sub>2</sub> with Features Larger than 10 <sup>4</sup> μm <sup>2</sup> Directly from Multilayer Sources. ACS Applied Electronic Materials, 2019, 1, 407-416.	2.0	23
207	Tandem Electrocatalytic CO <sub>2</sub> Reduction with Efficient Intermediate Conversion over Pyramid-Textured Cu–Ag Catalysts. ACS Applied Materials & Interfaces, 2021, 13, 40513-40521.	4.0	23
208	Reversible Photochromism in ⟠110⟩ Oriented Layered Halide Perovskite. ACS Nano, 2022, 16, 2942-2952.	7.3	23
209	Site dependence of large oxygen isotope effect inY0.7Pr0.3Ba2Cu3O6.97. Physical Review B, 1996, 54, 14982-14985.	1.1	22
210	Optical bleaching effect in InN epitaxial layers. Applied Physics Letters, 2006, 88, 191109.	1.5	22
211	Structural properties of Ge nanocrystals embedded in sapphire. Journal of Applied Physics, 2006, 100, 114317.	1.1	22
212	Membraneless laminar flow cell for electrocatalytic CO <sub>2</sub> reduction with liquid product separation. Journal Physics D: Applied Physics, 2017, 50, 154006.	1.3	22
213	Combined surface characterization and tribological (friction and wear) studies of CVD diamond films. Journal of Materials Research, 1993, 8, 2577-2586.	1.2	21
214	Quantitative stress mapping in alumina composites by optical fluorescence imaging. Acta Materialia, 1996, 44, 625-641.	3.8	21
215	Compositional modulation in InxGa1â^'xN: TEM and X-ray studies. Microscopy (Oxford, England), 2005, 54, 243-250.	0.7	21
216	High optical quality polycrystalline indium phosphide grown on metal substrates by metalorganic chemical vapor deposition. Journal of Applied Physics, 2012, 111, 123112.	1.1	21

#	Article	IF	CITATIONS
217	Thermal conductivity of isotopically controlled silicon nanostructures. New Journal of Physics, 2014, 16, 015021.	1.2	21
218	Compliant substrate epitaxy: Au on <mml:math xmlns:mml="http://www.w3.org/1998/Math/MathML"&gt;<mml:msub><mml:mi>MoS</mml:mi><mml:mn>2Physical Review B, 2016, 93, .</mml:mn></mml:msub></mml:math 	nl:m <b>n.ı</b> <td>m<b>l:mքs</b>ub&gt;</td>	m <b>l:mքs</b> ub>
219	Operando Investigation of Mn <sub>3</sub> O <sub>4+δ</sub> Co-catalyst on Fe <sub>2</sub> O <sub>3</sub> Photoanode: Manganese-Valency-Determined Enhancement at Varied Potentials. ACS Applied Energy Materials, 2018, 1, 814-821.	2.5	21
220	Ultrahigh thermal conductivity of isotopically enriched silicon. Journal of Applied Physics, 2018, 123, .	1.1	21
221	Scientific and Technological Assessment of Iron Pyrite for Use in Solar Devices. Energy Technology, 2018, 6, 8-20.	1.8	21
222	Surface Reconstruction of Perovskites for Water Oxidation: The Role of Initial Oxides' Bulk Chemistry. Small Science, 2022, 2, 2100048.	5.8	21
223	Mechanical Properties of Amorphous Hard Carbon Films Prepared by Cathodic ARC Deposition. Materials Research Society Symposia Proceedings, 1995, 383, 453.	0.1	20
224	Integrated microfluidic test-bed for energy conversion devices. Physical Chemistry Chemical Physics, 2013, 15, 7050.	1.3	20
225	PN junction rectification in electrolyte gated Mg-doped InN. Applied Physics Letters, 2011, 99, .	1.5	19
226	High figure-of-merit <i>p</i> -type transparent conductor, Cu alloyed ZnS <i>via</i> radio frequency magnetron sputtering. Journal Physics D: Applied Physics, 2017, 50, 505107.	1.3	19
227	Measuring the Edge Recombination Velocity of Monolayer Semiconductors. Nano Letters, 2017, 17, 5356-5360.	4.5	19
228	Raman intensities and interference effects for thin films adsorbed on metals. Journal of Chemical Physics, 1990, 92, 2067-2076.	1.2	18
229	Electrical and optical properties of GaN/Al2O3interfaces. Journal of Physics Condensed Matter, 2002, 14, 13337-13344.	0.7	18
230	Effect of native defects on optical properties of InxGa1â^'xN alloys. Applied Physics Letters, 2005, 87, 161905.	1.5	18
231	Isotopically engineered semiconductors: from the bulk to nanostructures. Physica Status Solidi (A) Applications and Materials Science, 2006, 203, 3550-3558.	0.8	18
232	Epitaxial growth of CdSexTe1â^'x thin films on Si(100) by molecular beam epitaxy using lattice mismatch graded structures. Journal of Crystal Growth, 2008, 310, 1081-1087.	0.7	18
233	Theory of thin-film-mediated exfoliation of van der Waals bonded layered materials. Physical Review Materials, 2018, 2, .	0.9	18
234	The kinetics of NaO + O <sub>2</sub> + M and NaO + CO <sub>2</sub> + M and their role in atmospheric sodium chemistry. Geophysical Research Letters, 1986, 13, 1395-1398.	1.5	17

#	Article	IF	CITATIONS
235	Effect of pretreatment process parameters on diamond nucleation on unscratched silicon substrates coated with amorphous carbon films. Journal of Applied Physics, 1996, 79, 485-492.	1.1	17
236	Theory of Nanocluster Size Distributions from Ion Beam Synthesis. Physical Review Letters, 2009, 102, 146101.	2.9	17
237	Structure map for embedded binary alloy nanocrystals. Applied Physics Letters, 2008, 93, 193114.	1.5	16
238	Molecular beam epitaxy of InGaN thin films on Si(111): Effect of substrate nitridation. Thin Solid Films, 2009, 517, 6512-6515.	0.8	16
239	Solar-Driven Gas-Phase Moisture to Hydrogen with Zero Bias. ACS Nano, 2021, 15, 19119-19127.	7.3	16
240	Giant Isotope Effect of Thermal Conductivity in Silicon Nanowires. Physical Review Letters, 2022, 128, 085901.	2.9	16
241	High quality InxGa1-xN thin films with x > 0.2 grown on silicon. Physica Status Solidi (B): Basic Research, 2010, 247, 1747-1749.	0.7	15
242	Near-band-edge photoluminescence emission in AlxGa1â^'xN under high pressure. Applied Physics Letters, 1998, 72, 2274-2276.	1.5	14
243	A Schottky topâ€gated twoâ€dimensional electron system in a nuclear spin free Si/SiGe heterostructure. Physica Status Solidi - Rapid Research Letters, 2009, 3, 61-63.	1.2	14
244	Si in GaN — On the Nature of the Background Donor. Physica Status Solidi (B): Basic Research, 1996, 198, 243-249.	0.7	13
245	DX-like behavior of oxygen in GaN. Physica B: Condensed Matter, 2001, 302-303, 23-38.	1.3	13
246	Band anticrossing effects in MgyZn1â^'yTe1â^'xSex alloys. Applied Physics Letters, 2002, 80, 34-36.	1.5	13
247	Strategies for integration of donor electron spin qubits in silicon. Microelectronic Engineering, 2006, 83, 1814-1817.	1.1	13
248	Dopants and defects in InN and InGaN alloys. Journal of Crystal Growth, 2006, 288, 278-282.	0.7	13
249	Homogeneous linewidth of the P31 bound exciton transition in silicon. Applied Physics Letters, 2009, 95, .	1.5	13
250	Semiconductor thin films directly from minerals—study of structural, optical, and transport characteristics of Cu2O thin films from malachite mineral and synthetic CuO. Thin Solid Films, 2012, 520, 3914-3917.	0.8	13
251	P-type InGaN across the entire alloy composition range. Applied Physics Letters, 2013, 102, 102111.	1.5	13
252	Thinâ€Film Solar Cells with InP Absorber Layers Directly Grown on Nonepitaxial Metal Substrates. Advanced Energy Materials, 2015, 5, 1501337.	10.2	13

#	Article	IF	CITATIONS
253	Initial Application of Selectedâ€lon Flowâ€Tube Mass Spectrometry to Realâ€Time Product Detection in Electrochemical CO <sub>2</sub> Reduction. Energy Technology, 2018, 6, 110-121.	1.8	13
254	Increased electrical activation in the near-surface region of sulfur and nitrogen coimplanted GaAs. Applied Physics Letters, 2000, 77, 3607-3609.	1.5	12
255	Photoluminescence of energetic particle-irradiated InxGa1â^'xN alloys. Applied Physics Letters, 2006, 88, 151101.	1.5	12
256	High-Resolution Raman and Luminescence Spectroscopy of Isotope-Pure <sup>28</sup> Si <sup>12</sup> C, Natural and <sup>13</sup> C – Enriched 4H-SiC. Materials Science Forum, 0, 778-780, 471-474.	0.3	12
25 <b>7</b>	Increased Optoelectronic Quality and Uniformity of Hydrogenated p-InP Thin Films. Chemistry of Materials, 2016, 28, 4602-4607.	3.2	12
258	Deterministic Assembly of Arrays of Lithographically Defined WS2 and MoS2 Monolayer Features Directly From Multilayer Sources Into Van Der Waals Heterostructures. Journal of Micro and Nano-Manufacturing, 2019, 7, .	0.8	12
259	High dose Cl implantation in ZnSe: Impurity incorporation and radiation damage. Journal of Applied Physics, 1994, 75, 1378-1383.	1.1	11
260	Comparison study of photoluminescence from InGaN/GaN multiple quantum wells and InGaN epitaxial layers under large hydrostatic pressure. Applied Physics Letters, 1998, 73, 1613-1615.	1.5	11
261	Electrical and electrothermal transport in InN: The roles of defects. Physica B: Condensed Matter, 2009, 404, 4862-4865.	1.3	11
262	A direct comparison of non-destructive techniques for determining bridging stress distributions. Journal of the Mechanics and Physics of Solids, 2012, 60, 1462-1477.	2.3	11
263	Techno-economic assessment of emerging CO2 electrolysis technologies. STAR Protocols, 2021, 2, 100889.	0.5	11
264	Effects of pressure on the band structure of highly mismatched Zn1â^'yMnyOxTe1â^'x alloys. Applied Physics Letters, 2004, 84, 924-926.	1.5	10
265	InGaN Thin Films Grown by ENABLE and MBE Techniques on Silicon Substrates. Materials Research Society Symposia Proceedings, 2008, 1068, 1.	0.1	10
266	Fatigue threshold R-curves predict small crack fatigue behavior of bridging toughened materials. Acta Materialia, 2011, 59, 7654-7661.	3.8	10
267	Photovoltaic action from In <sub>x</sub> Ga <sub>1â€x</sub> N pâ€n junctions with x > 0.2 grown on silicon. Physica Status Solidi C: Current Topics in Solid State Physics, 2011, 8, 2466-2468.	0.8	10
268	Pressure-induced structural transition of CdxZn1â^'xO alloys. Applied Physics Letters, 2016, 108, .	1.5	10
269	Minor Product Polymerization Causes Failure of High-Current CO <sub>2</sub> -to-Ethylene Electrolyzers. ACS Energy Letters, 2022, 7, 599-601.	8.8	10
270	Elucidating Reaction Pathways of the CO <sub>2</sub> Electroreduction via Tailorable Tortuosities and Oxidation States of Cu Nanostructures. Advanced Functional Materials, 2022, 32, .	7.8	9

#	Article	IF	CITATIONS
271	Diamond growth on silicon nitride by microwave plasma chemical vapor deposition. Diamond and Related Materials, 1992, 1, 818-823.	1.8	8
272	Laboratory studies of gas phase sodium diffusion. Journal of Chemical Physics, 1986, 85, 3469-3475.	1.2	7
273	The effect of coimplantation on the electrical activity of implanted carbon in GaAs. Journal of Applied Physics, 1993, 74, 7118-7123.	1.1	7
274	Spatially resolved measurement of lattice damage in alphaâ€particleâ€irradiated type IIa natural diamond by confocal photoluminescence microscopy. Journal of Applied Physics, 1994, 76, 4050-4053.	1.1	7
275	Reversible phase changes in Ge–Au nanoparticles. Applied Physics Letters, 2011, 98, 193101.	1.5	7
276	Taming transport in InN. Physica Status Solidi (A) Applications and Materials Science, 2012, 209, 83-86.	0.8	7
277	Effects of surface diffusion in electrocatalytic CO2 reduction on Cu revealed by kinetic Monte Carlo simulations. Journal of Chemical Physics, 2021, 155, 164701.	1.2	7
278	Group III-nitride alloys as photovoltaic materials. , 2004, , .		6
279	Oxygen induced band-gap reduction in ZnOxSe1â^'x alloys. Physica Status Solidi (B): Basic Research, 2004, 241, 603-606.	0.7	6
280	Pressure dependence of optical transitions in semiconducting single-walled carbon nanotubes. Physica Status Solidi (B): Basic Research, 2004, 241, 3367-3373.	0.7	6
281	Photoluminescence enhancement of Er-doped silica containing Ge nanoclusters. Applied Physics Letters, 2009, 95, .	1.5	6
282	Processing route for size distribution narrowing of ion beam synthesized nanoclusters. Applied Physics Letters, 2009, 95, 083120.	1.5	6
283	Atomic and electronic structures of lattice mismatched Cu2O/TiO2 interfaces. Applied Physics Letters, 2014, 104, 211605.	1.5	6
284	Surface origin and control of resonance Raman scattering and surface band gap in indium nitride. Journal Physics D: Applied Physics, 2016, 49, 255102.	1.3	6
285	Copper sulfide as the cation exchange template for synthesis of bimetallic catalysts for CO <sub>2</sub> electroreduction. RSC Advances, 2021, 11, 23948-23959.	1.7	6
286	Design principles of tandem cascade photoelectrochemical devices. Sustainable Energy and Fuels, 2021, 5, 6361-6371.	2.5	6
287	Diamond growth on hard carbon films. Diamond and Related Materials, 1996, 5, 1080-1086.	1.8	5
288	Electron Transport Properties of InN. Materials Research Society Symposia Proceedings, 2005, 892, 91.	0.1	5

#	Article	IF	CITATIONS
289	Highly luminescent InxGa1-xN thin films grown over the entire composition range by energetic neutral atom beam lithography & epitaxy (ENABLE). Physica Status Solidi C: Current Topics in Solid State Physics, 2009, 6, S409-S412.	0.8	5
290	Electrical Properties of Natural Iia Diamonds Using Photo- and Particle Excitation. Materials Research Society Symposia Proceedings, 1993, 302, 245.	0.1	4
291	Evolution of crystallinity of GaN layers grown at low temperature on sapphire with dimethylhydrazine and triethylgallium. Journal of Crystal Growth, 2001, 231, 89-94.	0.7	4
292	Pressure-dependent photoluminescence study of CuGaSe2. Physica Status Solidi (B): Basic Research, 2004, 241, 3117-3122.	0.7	4
293	Evaluation of exhaled nitric oxide measurements in the emergency department for patients with acute asthma. Annals of Allergy, Asthma and Immunology, 2008, 100, 415-419.	0.5	4
294	Stacking faults and phase changes in Mg-doped InGaN grown on Si. Physica Status Solidi C: Current Topics in Solid State Physics, 2009, 6, S421-S424.	0.8	4
295	Progress in Semiconductor Spectroscopy Using Isotopically Enriched Si. AIP Conference Proceedings, 2005, , .	0.3	3
296	Progress on III-nitride/silicon hybrid multijunction solar cells. , 2010, , .		3
297	Nucleation of melting and solidification in confined high aspect ratio thin films. Journal of Applied Physics, 2017, 122, 105304.	1.1	3
298	The Bright Side and Dark Side of Hybrid Organic–Inorganic Perovskites. Journal of Physical Chemistry C, 2020, 124, 27340-27355.	1.5	3
299	The nitrogen-hydrogen complex in ZnSe. Journal of Crystal Growth, 1994, 138, 1071-1072.	0.7	2
300	Performance of Ultra Hard Carbon Wear Coatings on Microgears Fabricated by Liga. Materials Research Society Symposia Proceedings, 1998, 546, 115.	0.1	2
301	Analysis of Nanoscale Stress in Strained Silicon Materials and Microelectronics Devices by Energy-Filtered Convergent Beam Electron Diffraction. ECS Transactions, 2006, 2, 559-568.	0.3	2
302	Kinetics of visible light photo-oxidation of Ge nanocrystals: Theory and in situ measurement. Applied Physics Letters, 2007, 90, 163118.	1.5	2
303	Shallow Impurity Absorption Spectroscopy in Isotopically Enriched Silicon. AIP Conference Proceedings, 2007, , .	0.3	2
304	Evidence for p-type InN. AIP Conference Proceedings, 2007, , .	0.3	2
305	Nuclear Polarization of Phosphorus Donors in [sup 28]Si by Selective Optical Pumping. AlP Conference Proceedings, 2010, , .	0.3	2
306	Modeling pulsed-laser melting of embedded semiconductor nanoparticles. Journal of Applied Physics, 2011, 110, 094307.	1.1	2

 $\mathsf{JOEL}\,\mathsf{W}\,\mathsf{AGER}$ 

#	Article	IF	CITATIONS
307	Photophysics of Localized Deep Defect States in Hybrid Organic–Inorganic Perovskites. Journal of Physical Chemistry C, 2021, 125, 6975-6982.	1.5	2
308	Effect of oxygen on the electronic band structure of II-O-VI alloys. , 2004, , .		1
309	Relation Between Structural and Optical Properties of InN and InxGa1â^'xN Thin Films. AIP Conference Proceedings, 2005, , .	0.3	1
310	Structural Characterization of GeSn Alloy Nanocrystals Embedded in SiO <sub>2</sub> . Materials Research Society Symposia Proceedings, 2009, 1184, 154.	0.1	1
311	Self-consistent mean-field theory of size distribution narrowing during ramped temperature ion beam synthesis. Journal of Applied Physics, 2013, 114, 234301.	1.1	1
312	Low-temperature synthesized, p-type transparent conducting material for PV devices. , 2015, , .		1
313	Theory of liquid-mediated strain release in two-dimensional materials. Physical Review Materials, 2022, 6, .	0.9	1
314	Reducing Dislocation Density by Sequential Implantation of Ge and C in Si. Materials Research Society Symposia Proceedings, 1993, 298, 139.	0.1	0
315	Characterization of Cvd Diamond Films by Optical Spectroscopies. Materials Research Society Symposia Proceedings, 1993, 302, 275.	0.1	0
316	Nickel, Morris, and Ager reply. Physical Review Letters, 1994, 72, 1389-1389.	2.9	0
317	Isotopic Effects in the Indirect Excitonic Transitions of Isotopically Enriched Silicon. AIP Conference Proceedings, 2005, , .	0.3	0
318	In Situ Characterization of Ge Nanocrystals Near the Growth Temperature. AIP Conference Proceedings, 2005, , .	0.3	0
319	A Chemical Approach to 3-D Lithographic Patterning of Si and Ge Nanocrystals. Materials Research Society Symposia Proceedings, 2005, 901, 1.	0.1	0
320	Analysis of Nano-scale Strain Near Shallow Trench Isolation Structures by Energy-filtered Convergent Beam Electron Diffraction. Microscopy and Microanalysis, 2006, 12, 938-939.	0.2	0
321	Defect Doping of InN. AIP Conference Proceedings, 2007, , .	0.3	0
322	Synthesis and Optical Properties of Multiband III-V Semiconductor Alloys. AIP Conference Proceedings, 2007, , .	0.3	0
323	Melting Kinetics of Confined Systems at the Nanoscale: Superheating and Supercooling. AIP Conference Proceedings, 2007, , .	0.3	0
324	My Modeling Nanocluster Formation During Ion Beam Synthesis. Materials Research Society Symposia Proceedings, 2009, 1181, 60.	0.1	0

#	Article	IF	CITATIONS
325	Solar fuels production by artificial photosynthesis. , 2013, , .		0
326	Interfacial free energies determined from binary embedded alloy nanocluster geometry. APL Materials, 2013, 1, 052105.	2.2	0
327	On the origin of photocarrier losses in Iron Pyrite nanocubes: Charge carrier dynamics and electrical transport study. , 2016, , .		0
328	(Invited) Solar-Driven Electrochemical Conversion of Carbon Dioxide to Hydrocarbons and Oxygenates. ECS Meeting Abstracts, 2017, , .	0.0	0
329	Energy Spotlight. ACS Energy Letters, 2022, 7, 1574-1576.	8.8	0